



Article

Direct Conversion of Bovine Dermal Fibroblasts into Myotubes by Viral Delivery of Transcription Factor bMyoD

Boram Son ^{1,†}, Seong Ho Lee ^{2,†}, Seyoung Hong ², Miji Kwon ², Jinmyoung Joo ³ , Kwang Suk Lim ^{2,*} and Hee Ho Park ^{1,4,*} 

¹ Department of Bioengineering, Hanyang University, Seoul 04763, Korea; boramson@hanyang.ac.kr

² Department of Smart Health Science and Technology, Kangwon National University, Chuncheon 24341, Korea; tjdgh020393@kangwon.ac.kr (S.H.L.); syh@kangwon.ac.kr (S.H.); alwl5519@kangwon.ac.kr (M.K.)

³ Department of Biomedical Engineering, Ulsan National Institute of Science and Technology (UNIST), Ulsan 44919, Korea; jjoo@unist.ac.kr

⁴ Education and Research Group for Biopharmaceutical Innovation Leader, Hanyang University, Seoul 04763, Korea

* Correspondence: kslim@kangwon.ac.kr (K.S.L.); parkhh@hanyang.ac.kr (H.H.P.); Tel.: +82-33-250-6279 (K.S.L.); +82-2-2220-0497 (H.H.P.)

† These authors contributed equally to this work.

Abstract: Direct reprogramming of somatic cells to myoblasts and myotubes holds great potential for muscle development, disease modeling and regenerative medicine. According to recent studies, direct conversion of fibroblasts to myoblasts was performed by using a transcription factor, myoblast determination protein (MyoD), which belongs to a family of myogenic regulatory factors. Therefore, MyoD is considered to be a key driver in the generation of induced myoblasts. In this study, we compared the direct phenotypic conversion of bovine dermal fibroblasts (BDFs) into myoblasts and myotubes by supplementing a transcription factor, bovine MyoD (bMyoD), in the form of recombinant protein or the bMyoD gene, through retroviral vectors. As a result, the delivery of the bMyoD gene to BDFs was more efficient for inducing reprogramming, resulting in direct conversion to myoblasts and myotubes, when compared with protein delivery. BDFs cultured with retrovirus encoding bMyoD increased myogenic gene expression, such as MyoG, MYH3 and MYMK. In addition, the cells expressed myoblast or myotube-specific marker proteins, MyoG and Desmin, respectively. Our findings provide an informative tool for the myogenesis of domestic-animal-derived somatic cells via transgenic technology. By using this method, a new era of regenerative medicine and cultured meat is expected.

Keywords: direct conversion; bovine MyoD (bMyoD); bovine dermal fibroblasts (BDFs); bovine myoblasts; bovine myotubes



Citation: Son, B.; Lee, S.H.; Hong, S.; Kwon, M.; Joo, J.; Lim, K.S.; Park, H.H. Direct Conversion of Bovine Dermal Fibroblasts into Myotubes by Viral Delivery of Transcription Factor bMyoD. *Appl. Sci.* **2022**, *12*, 4688. <https://doi.org/10.3390/app12094688>

Academic Editor: Neill Turner

Received: 30 March 2022

Accepted: 5 May 2022

Published: 6 May 2022

Publisher's Note: MDPI stays neutral with regard to jurisdictional claims in published maps and institutional affiliations.



Copyright: © 2022 by the authors. Licensee MDPI, Basel, Switzerland. This article is an open access article distributed under the terms and conditions of the Creative Commons Attribution (CC BY) license (<https://creativecommons.org/licenses/by/4.0/>).

1. Introduction

Skeletal muscles are composed of myofibers, connective tissues, vessels and nerves, and this group of various tissues makes the muscles move physically [1]. When the skeletal muscles have been damaged, they could be cured and renewed as follows. If minor muscle damage happens, local inflammation triggers the release of various biological factors. Some growth factors, such as hepatocyte growth factor (HGF) and insulin-like growth factor (IGF), can modulate the proliferation and differentiation of satellite cells (SCs) and myoblasts. This result can be explained due to the reaction in muscle tissue homeostasis and regeneration by these growth factors [2,3]. In addition, growth factors that do not target muscle cells, such as vascular endothelial growth factor (VEGF) and nerve growth factor (NGF), are also essential for muscle maturation and regeneration [4–6]. After release of the growth factors, related signaling pathways are activated, leading to

recruitment, expansion, and differentiation in the muscle stem cells, resulting in muscle fiber regeneration for damaged tissues [7]. In detail, the pro-inflammatory cytokines, such as TNF- α and IL-1 β , and the anti-inflammatory cytokine represented as IL-10, enhance not only the proliferation but also differentiation of myoblasts. Then, cell signaling pathways (e.g., p38MAPK or NF- κ B) are initiated and activated by those cytokines. Cytokines, such as TNF- α , may regulate muscle cells during early phases of muscle regeneration through their effects on pro-inflammatory macrophages and also influence muscle cells more directly by binding their receptors on the cells in the later phases. However, serious physical damage, such as from car accidents, explosive injuries, and iatrogenic disorders, can cause volumetric muscle loss (VML) [8]. It could induce insufficient muscle stem cell recruitment and, thus, serious damage to the endogenous self-repair system, resulting in non-functional scarring. Currently, therapy of the VML is considered to be a major challenge, since the conventional treatment method, injection of autonomous muscle cells, has limitations in practical treatment, due to the unstable supply of muscle tissues and significant donor site morbidity [9]. Therefore, it is essential to have efficient techniques to solve the problems of conventional methods.

In the field of therapeutic approaches for tissue regeneration, effective treatments for the damaged skeletal muscles include clinical applications with multi-potent stem cells, such as SCs, myoblast or muscle-derived stem cells (MDSCs), and mesenchymal stem cells (MSCs) [10–12]. Therefore, it has become more significant to regulate differentiation of the multi-potent stem cells, using biochemical factors, represented as growth factors or other biomolecules [13,14], and biophysical factors, such as mechanical or electrical stimulations [15–19]. Moreover, using biochemical factors combined with biophysical factors has been suggested as a useful method for the control of stem cell differentiation. Growth factors can be treated by systematic injection methods, bio-scaffold, and drug delivery systems [20–22]. Despite these improved methods, it is still difficult and inefficient to regulate stem cell fate into intended lineages delicately. In addition, the use of stem cells cannot be free from high cost and supply problems [23].

Recently, researchers discovered new types of cells, which can alternate existing stem cells, induced pluripotent stem cells (iPSCs) or directly reprogrammed somatic cells [24,25]. In 2006, Yamanaka and Takahashi induced the reprogramming of murine and human fibroblasts, resulting in the generation of iPSCs with self-renewal and pluripotent abilities. Following the discovery of iPSCs, numerous studies accelerated research related to the direct reprogramming of somatic cells (also known as direct conversion) of somatic cells into other types of somatic cells, through various approaches, such as genetic modification, biomaterials, growth factors, small molecules, and cocktail methods [26,27]. As a result of this direct reprogramming, somatic cells can be differentiated into specific cells without going through the intermediate pluripotent stage. Therefore, direct conversion by various transcription factors and biomolecules can be considered as a promising strategy for regenerative medicine, since it bypasses the intermediate pluripotent stage and, thus, the required time can be reduced in clinical applications [5,28]. Therefore, direct conversion is applied for differentiating fibroblasts into various somatic cells, such as cardiomyocytes [29,30], neurons [31,32], chondrocytes [33,34], myoblasts and myotubes [35,36], and more.

To induce direct reprogramming of the somatic cells into intended types of cells, transcription factors are delivered through various methods. According to recent studies, the protein-based approaches, using cell-penetrating peptides or proteins for direct conversion of somatic cells, have been found to be practical and suitable for clinical use with a low risk of genomic integration [37–40]. Regarding the viral-based approaches, using retrovirus and lentivirus for direct conversion of somatic cells has been found to be practical in terms of high efficiency [41,42]. However, those studies are limited in *in vitro* results utilizing human cells and, thus, direct conversion in other species, such as bovine-derived somatic cells, remain relatively unexplored, which is an obstacle in research for domestic animal applications.

In this study, we tried to determine an efficient method for the direct conversion of bovine dermal fibroblasts (BDFs) into myogenic cells using a transcription factor, bovine myoblast determination protein (bMyoD), comparing a protein-based method and retrovirus-based method. Therefore, we performed genetical and immunocytochemical analysis to investigate the direct reprogramming of cells in the early stage (myoblasts) and late stage (myotube) of myogenesis [43,44]. It is anticipated that this genetic engineering strategy, with high efficiency, could be a useful tool for regenerative therapy for muscle-related diseases, such as sarcopenia or cachexia [45]. In addition, if sufficient efficiency can be achieved with the transgene-based approach without chromosomal integration, such cell-based therapies would be beneficial in food industries for the generation of cultured meat products [46,47].

2. Materials and Methods

2.1. Cell Culture

BDFs (#B2300, ScienCell Research Laboratories, Carlsbad, CA, USA) were maintained by Dulbecco's Modified Eagle's Medium (DMEM; HyClone, Logan, UT, USA) supplemented with 10% fetal bovine serum (Gibco, Waltham, MA, USA), 100 U/mL penicillin, and 100 µg/mL streptomycin (Gibco) in 5% CO₂ humidified incubator at 37 °C. When the confluence reached about 80%, BDFs were transferred in a 1:6 ratio. BDFs used in this study were under passage 10 in all experimental steps.

2.2. Plasmid Construction and Production of 30Kc19-bMyoD-NLS-R9 (30MNR)

The 30Kc19-bMyoD-NLS-R9 (30MNR) protein (NLS sequence: KKKRKY) was produced similarly as described in our previous studies [48–52]. Briefly, bMyoD gene was synthesized (Cosmo Genetech, Seoul, Korea) and then pET23a/30MNR was constructed by inserting cDNA of bMyoD between *NheI* and *XhoI* sites of pET23a expression vector (Novagen, Madison, WI, USA) with a T7-tag at the N-terminus and a 6 × His-tag at the C-terminus. The fusion protein was produced using vector-transformed *E. coli*, BL21 (Novagen). Cells were cultured in LB medium containing 100 µg/mL ampicillin at 37 °C and induced with isopropyl- α -D-thiogalactopyranoside (IPTG, 1 mM). After further incubation at 37 °C for 4 h, cells were harvested and then disrupted by ultrasonication. Soluble protein was purified from the supernatant using HisTrap HP column (GE Healthcare, Uppsala, Sweden) and dialyzed with Tris-HCl buffer (pH 8.0) using desalting column (GE Healthcare). Final purity of fusion protein was higher than 90%. Purified proteins were stored at –70 °C. Micro BCA kit (Thermo Fisher Scientific Inc., Rockford, IL, USA) was used to perform quantitative analysis of the proteins.

2.3. SDS-PAGE and Immunoblot Analysis

Reducing SDS-PAGE (12% polyacrylamide gel) was performed. Samples were mixed with reducing sample buffer containing SDS and β -mercaptoethanol (BME) (pH 6.8) followed by denaturation by boiling. After electrophoresis, each sample was separated in accordance with size. The polyacrylamide gel was immersed in Coomassie blue staining solution, followed by destaining for analysis.

2.4. Cell-Penetration Assay

A confocal microscope (EZ-C1, Nikon, Tokyo, Japan) was used to visualize cellular uptake of fusion protein. As such, 4×10^4 cells of BDFs were seeded onto a well of 24-well plates and incubated at 37 °C overnight. Fusion protein at concentration of 80 µg/mL was added to BDFs and then incubated at 37 °C for another 24 h. After washing with PBS several times, Hoechst 33342 was used to stain nuclei for 10 min. Live cell images were taken using the manufacturer's software (Nikon).

2.5. Retrovirus Production, Titration, and Transduction

Retroviral vector supernatants were generated by co-transfecting 10 µg of retroviral transfer vector, and 5 µg of vesicular stomatitis virus (VSV-G) packaging plasmids into GP2-293 cells in a 100 mm dish using 4X linear PEI reagent. Supernatants were collected at 48 h after transfection and filtered through a 0.45-µm polyvinylidene fluoride (PVDF) syringe filter (Corning Life Sciences, Tewksbury, MA, USA). Then the virus was concentrated using 22,000 rpm ultracentrifugation at 4 °C for 2 h. To determine the titer, 1×10^5 HT1080 cells in a 6-well plate were infected with serial dilutions of the retroviral vector supernatants in the presence of polybrene (8 mg/mL) (Sigma-Aldrich, St. Louis, MO, USA) and analyzed 3 days before transduction by flow cytometry analysis (FACS; BD Biosciences, San Jose, CA, USA). Transduction of BDFs was performed on 5×10^4 cells per 24-well plate.

2.6. RNA Isolation, cDNA Synthesis, and Reverse Transcription Polymerase Chain Reaction (RT-PCR)

The cells were disrupted using 1 mL of TRIzol (Sigma) per 5×10^6 cells. After addition of 200 µL of chloroform, cells were centrifuged at $12,000 \times g$ for 15 min at 4 °C. An upper aqueous phase was collected and mixed with isopropyl alcohol. After centrifugation at $12,000 \times g$ for 10 min, the supernatant was removed, and the pellet was washed with 75% ethanol. The synthesis of cDNA was conducted using the M-MLV cDNA synthesis kit (Enzymomics, Daejeon, Korea) according to the manufacturer's instructions. Reverse transcription polymerase chain reaction (RT-PCR) was carried out with AccuPower® PCR Premix (Bioneer, Daejeon, Korea).

2.7. Immunocytochemical Analysis

For immunocytochemical analysis, the cells were fixed with 4% paraformaldehyde (Sigma-Aldrich) for 15 min and permeabilized with 0.05% Tween-20 (Amresco, Cleveland, OH, USA) for 2 h. Anti-MyoD (Abcam, Cambridge, UK), anti-MyoG (Abcam), and anti-Desmin (Carlsbad, CA, USA) was used as primary antibody (1:100). Anti-mouse Alexa 594-conjugated secondary antibody (1:250) was used for MyoD, and anti-rabbit Alexa 488-conjugated secondary antibody (1:250) was used for MyoG and Desmin. Hoechst 33342 (Life Technologies, Gaithersburg, MD, USA) was used to stain the nuclei, followed by imaging with a fluorescence microscope (Olympus, Lake Success, NY, USA). The fluorescent images were quantified using ImageJ software.

2.8. Statistical Analysis

All the experiments were conducted in at least triplicate. Data are expressed as the mean \pm standard deviation (s.d.). Statistical significance was determined using the Student's *t*-test to compare two groups through SigmaPlot. For all experiments, statistical significance was represented by * for $p < 0.05$, ** for $p < 0.01$, and *** for $p < 0.001$.

3. Results

3.1. Soluble Expression and Purification of 30MNR Protein

To improve stability and soluble expression, the transcription factor, bMyoD, was conjugated with 30Kc19 and, thus, the 30Kc19-bMyoD-NLS-R9 (30MNR) gene was inserted into expression vector pET-23a (Figure 1A). The insertion of the 30MNR gene was confirmed by PCR (Figure 1B). The recombinant fusion protein, 30MNR, was expressed in *E. coli* and purified (Figure 1C). After purification of the 30MNR protein in the soluble fraction, SDS-PAGE analysis was performed (Figure 1D). A band of 30MNR protein with a size of about 70 kDa was observed in the soluble fraction.

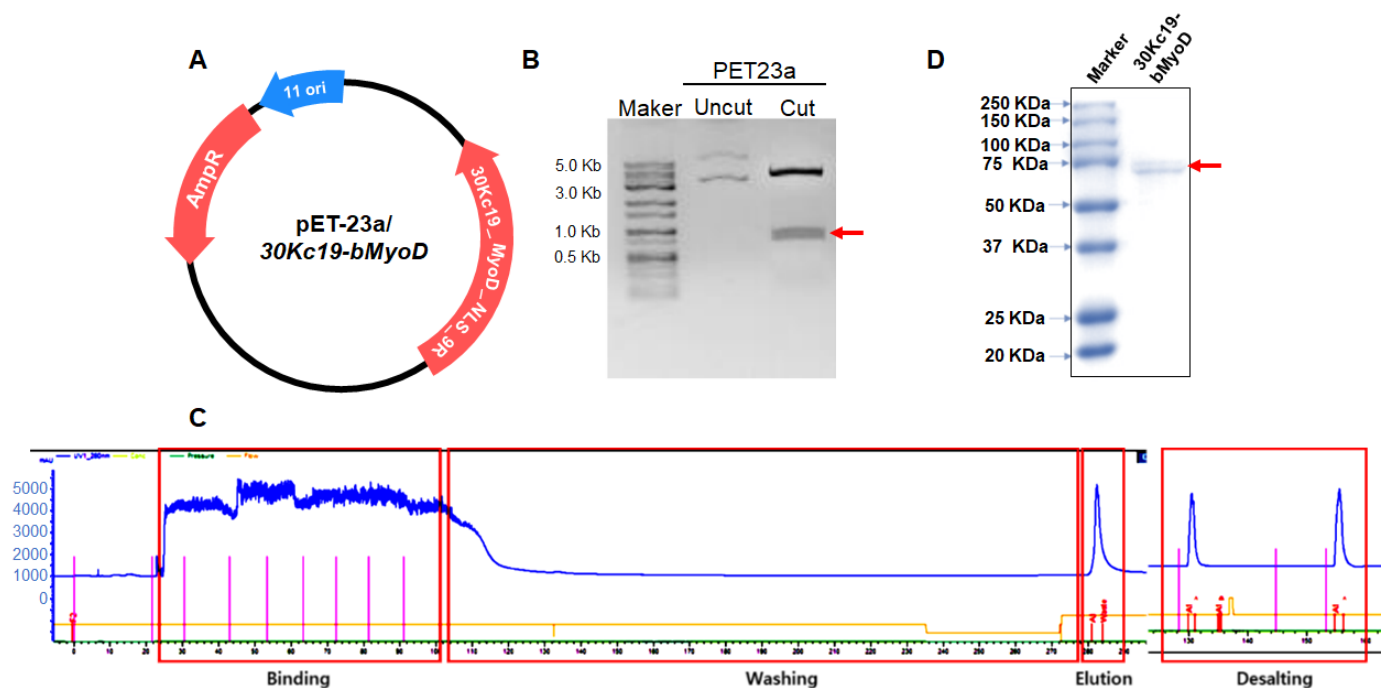


Figure 1. Gene construction and protein expression of 30MNR. (A) Construction of *E. coli* expression vector, pET–23a/30Kc19–bMyoD. (B) PCR gel for confirming gene cloning and double digestion of 30Kc19–bMyoD–NLS-R9 (30MNR). A red arrow indicates 30MNR gene. (C) Chromatogram tracing purified 30MNR protein after elution. (D) SDS-PAGE gel of purified 30MNR protein. A red arrow indicates purified 30MNR protein.

3.2. Intracellular Delivery but Inefficient Direct Reprogramming of 30MNR Protein

In order to analyze the cell-penetrating property and nuclear-localizing property of the transcription factor bMyoD conjugated with 30Kc19, R9, and NLS sequence, in the form of 30MNR protein, 50 µg/mL of 30MNR protein was treated with BDFs, followed by immunocytochemical analysis. The 30MNR protein was added to the BDFs every third day, regarding stability of the protein. On day 7, cells were analyzed by immunocytochemistry, and then observed with a confocal microscope. BDFs cultured with the 30MNR protein showed significant expression of bMyoD, indicated by red fluorescence, whereas the control (untreated cells) did not (Figure 2A,B). Therefore, intracellular delivery of bMyoD was confirmed in the form of 30MNR protein. Then, in order to induce the direct reprogramming of BDFs into myoblasts, 80 µg/mL of the 30MNR protein was treated with the BDFs. However, cells cultured with the 30MNR protein did not show obvious morphological change, such as long myotube formation, compared with the control (Figure 2C). In addition, the proliferation tendency of the BDFs was observed similarly, regardless of the 30MNR recombinant protein addition. Moreover, the BDFs cultured with the 30MNR protein did not express MyoG protein, indicated by green fluorescence (Figure 2D), demonstrating that protein-induced myogenesis was inefficient.

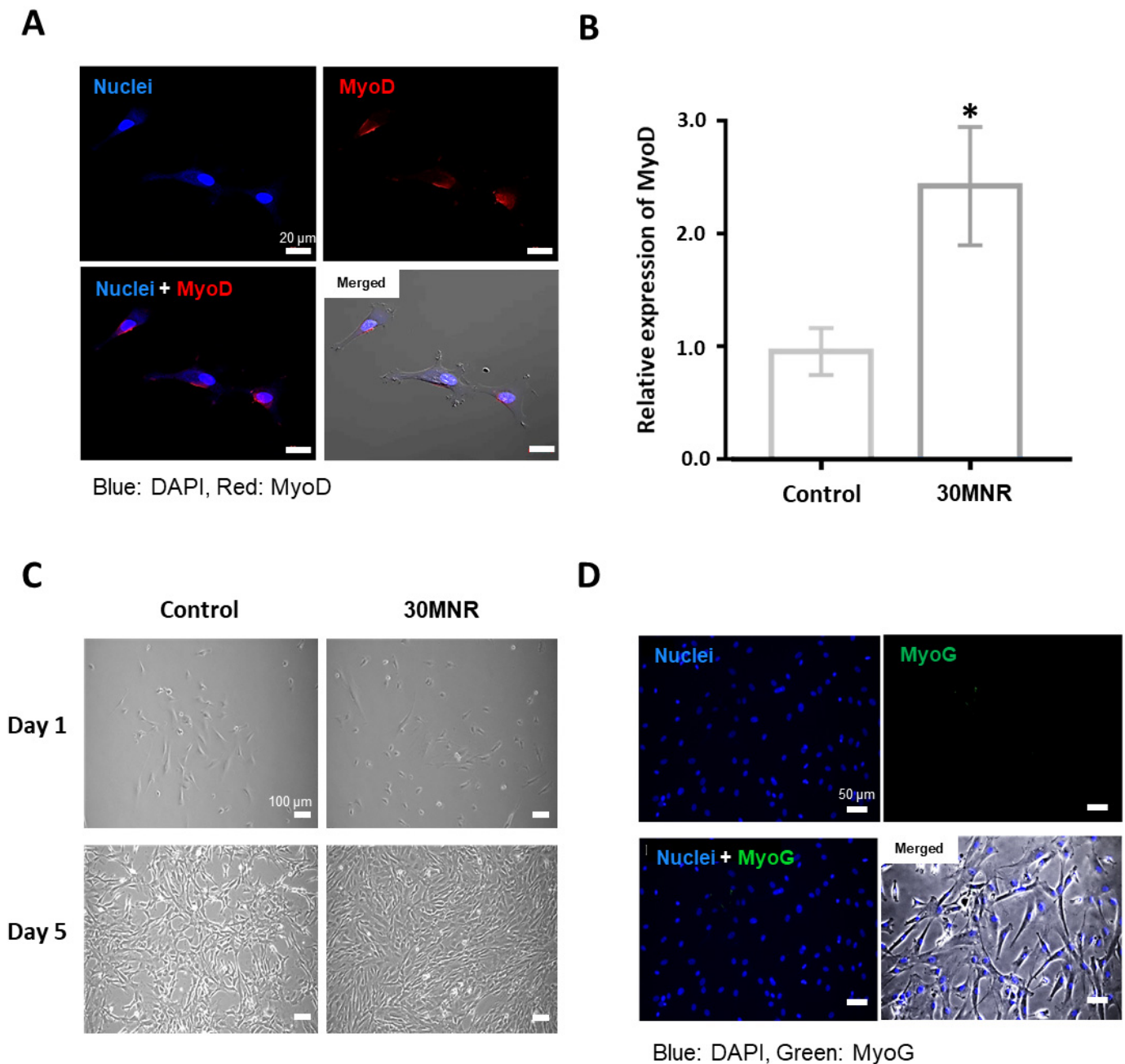


Figure 2. Protein-based direct reprogramming using 30Kc19-bMyoD-NLS-R9 (30MNR) protein. Intracellular delivery of the protein was observed; however, efficiency of reprogramming was not adequate in BDFs cultured with 30MNR protein. (A) Immunocytochemistry to confirm intracellular delivery of 30MNR fusion protein in BDFs. Further, 30MNR was indicated by red fluorescence. Scale bars, 20 μ m. (B) Quantified values of bMyoD fluorescence using Image J. $n = 3$ per group and statistical significance was determined using one-way ANOVA. * $p < 0.05$. (C) Morphology of cells observed after treatment with 80 μ g/mL of 30MLR fusion protein for 5 days. Scale bars, 100 μ m. (D) Immunocytochemistry to confirm expression of myogenic marker protein, MyoG. Scale bars, 50 μ m.

3.3. Production of bMyoD Encoding Retrovirus, RV/bMyoD

Genes of bMyoD or DsRed were inserted into a retroviral expression vector, pMX, between *NheI* and *XhoI* restriction sites, respectively (Figure 3A). The insertion of the bMyoD gene was confirmed by double digestion with *NheI* and *XhoI* enzymes (Figure 3B). We investigated the titer of the produced retrovirus from the harvested supernatant of

GP2-293 packaging cells, which were co-transfected by pMXs/*DsRed*, VSV-G and PEI complex. When we infected HT1080 cells with serial dilutions of the retroviral vector supernatants, 10-fold dilution of the concentrated virus resulted in about 6% positive cells (Figure 3C). As a result, we confirmed that the titer of the concentrated virus was 1.5×10^6 TU/mL (Figure 3D), and based on this, MOI 10 was used for the following direct conversion experiments.

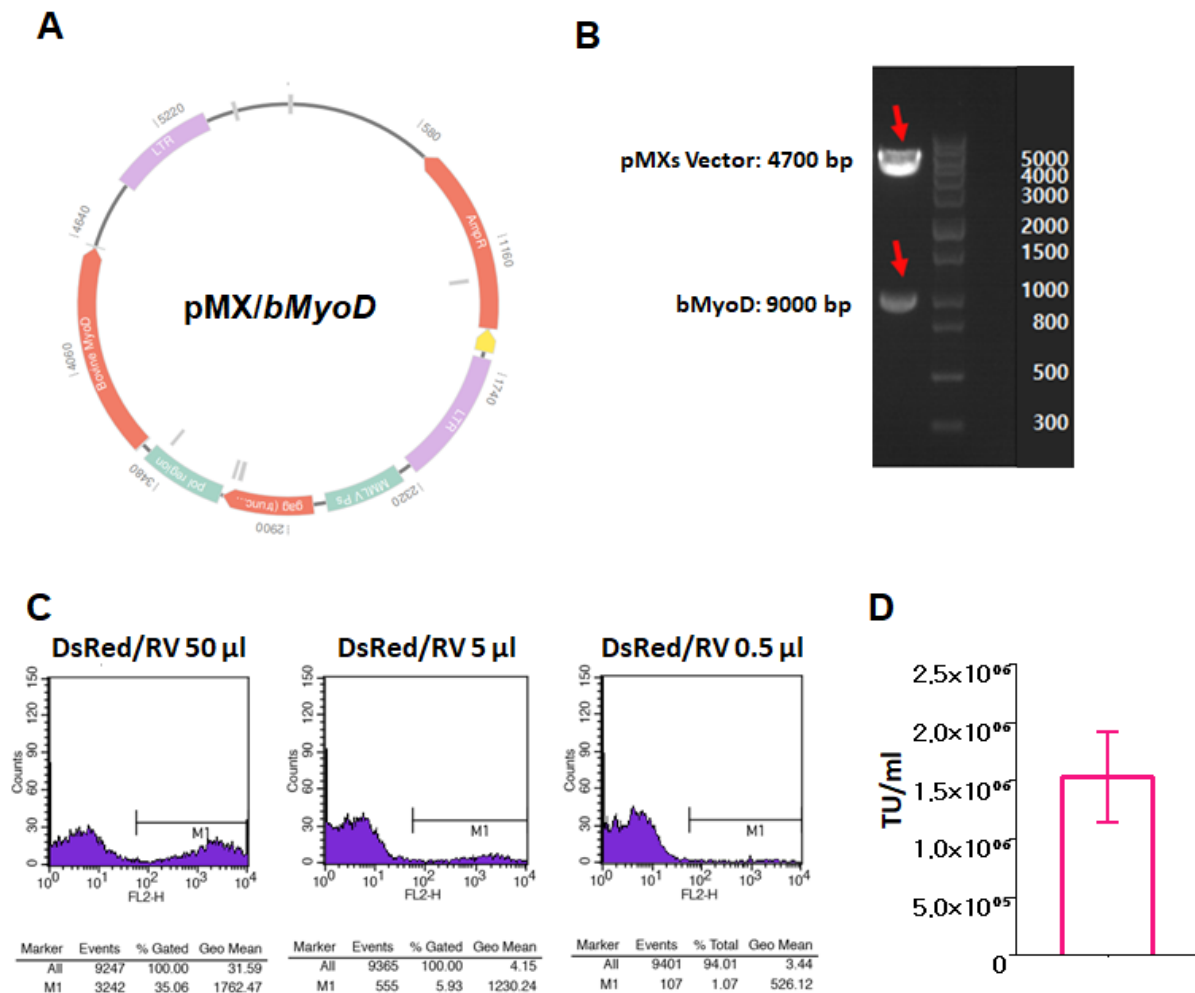


Figure 3. Viral-based direct reprogramming using bMyoD retrovirus. (A) Plasmid constructs of pMX/*bMyoD*. (B) PCR gel of double-digested pMX/*bMyoD* retroviral vector. Red arrows indicate pMX and bMyoD, respectively. (C) Histogram of FACS for infected HT1080 with concentrated retrovirus. (D) Titer of concentrated retrovirus. $n = 3$ per group.

3.4. Myogenic Gene Expression of Directly Reprogrammed Myogenic cells by RV/*bMyoD*

After 7 days of direct conversion of BDFs into myogenic cells using RV/*bMyoD*, morphological and genetical changes were analyzed (Figure 4). On day 3, the formation of myotubes in BDFs treated with RV/*bMyoD* was observed, showing elongated morphology, and more matured myotubes were generated over time (Figure 4A). Cells with parallel arrangements were also observed on days 3 and 5 after transduction with RV/*bMyoD*. Some of the cells showed fused and connected formation on day 5. On day 7, BDFs were analyzed for the expression of representative myogenic marker genes by RT-PCR (Figure 4B). Specific primers were used to detect the endogenous myogenin (*MyoG*), myosin heavy chain 3 (*MYH3*), and myomarker (*MYMK*). According to the results, BDFs with RV/*bMyoD* showed enhanced expression of those myogenic genes, whereas the control (untreated BDFs) did not show clear expression of the genes. Then, the intensity of each band was quantified using Image J, as shown in Figure 4C. As a reference gene, GAPDH

was used, by which each mRNA expression value was normalized. *RV/bMyoD*-treated BDFs showed a statistically significant increase in mRNA expression, compared with the value of control. Expression of *MyoG*, an early myoblast marker, was 4-fold to control. The expression of both *MYH3* and *MYMK*, the late myotube markers, was 7-fold to the control, respectively. The results demonstrated that *RV/bMyoD* treatment induces myogenesis of the BDFs, resulting in morphological changes and up-regulated expression of both an early myoblast gene and the late myotube genes.

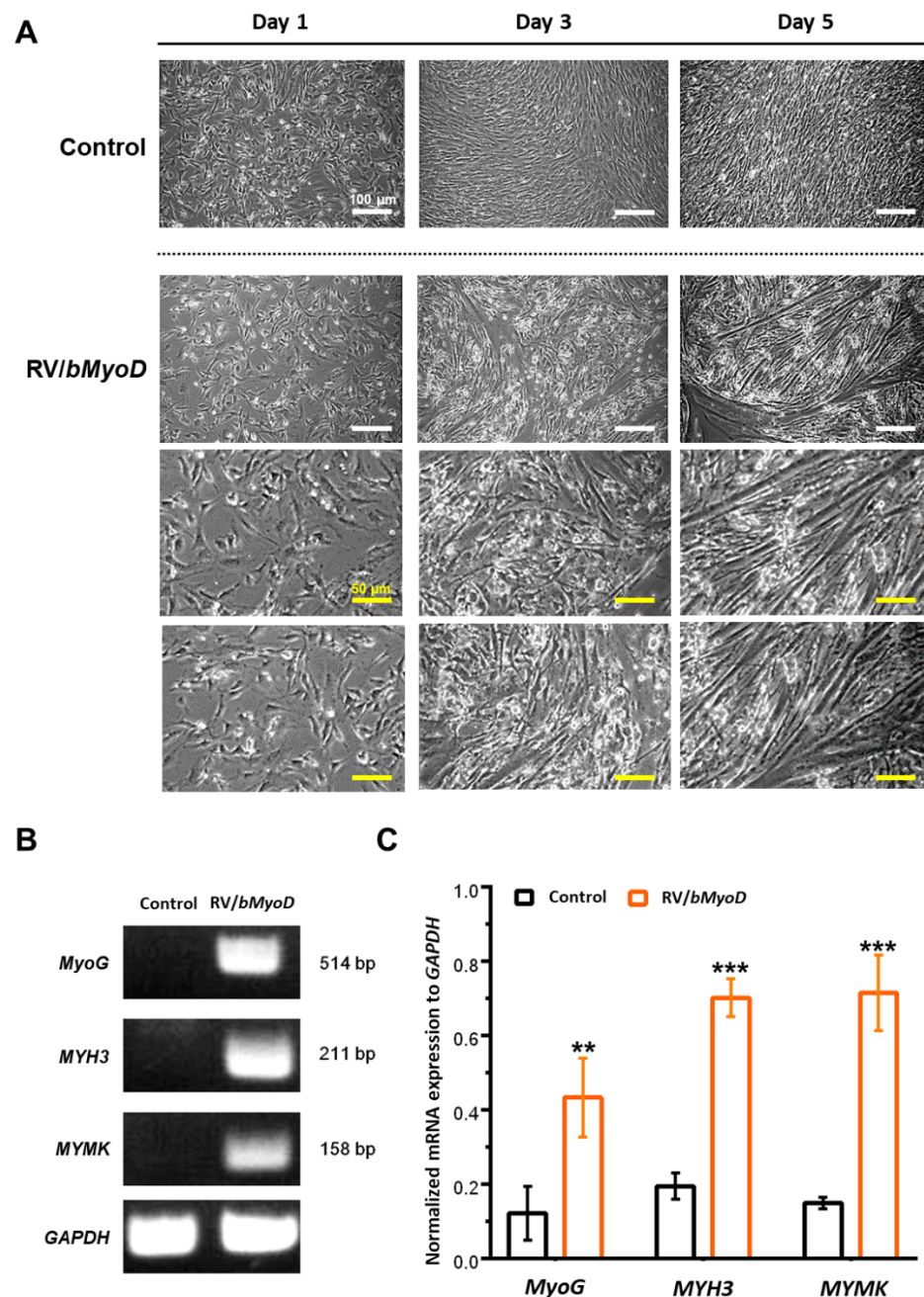


Figure 4. Observation of myotube formation and myogenic gene expression of induced myogenic cells. (A) Morphological analysis of BDFs. Induced myogenic cells using *RV/bMyoD* showed formation of microtubes. Scale bars, 100 μm in white and 50 μm in yellow. (B) PCR gel images of representative myogenic genes: *MyoG*, *MYH3*, *MYMK*. (C) Quantification of gene expression using Image J. $n = 3$ per group. Statistical significance was determined using one-way ANOVA in comparison with the non-treated control BDFs. ** $p < 0.01$, *** $p < 0.001$.

3.5. Myogenic Protein Expression of Directly Reprogrammed Myogenic Cells by RV/bMyoD

To further observe the efficiency of direct conversion using RV/bMyoD, the expression of representative myogenic proteins [53–55] was analyzed through immunocytochemistry (Figure 5). According to the results, RV/bMyoD-treated BDFs showed obviously increased expression of myogenic proteins, represented as MyoD, MyoG, and Desmin, compared with the control (Figure 5A,C,E). In addition, the morphology of the fluorescent cells was different from the original BDFs. Cells showed protrusions, connecting to neighboring cells, shown in Figure 5A. In Figure 5C,E, cells with green fluorescence were observed in the form of fused cells, which indicates myogenic morphology. Specifically, in Figure 5C, myotubes are observed clearly. The intensity of each fluorescence was quantified using ImageJ (Figure 5B,D,F). Directly reprogrammed myogenic cells with RV/bMyoD showed a statistically significant increase in the expression of all the proteins. The early myoblast marker proteins, such as MyoD and MyoG, showed 60-fold and 12.5-fold increases compared to each control, respectively (Figure 5B,D). Similarly, the late myotube marker protein, Desmin, showed a 35-fold increase compared to the control. As a result, RV/bMyoD treatment induced improvement in expression of early myoblast proteins and also, late myotube proteins, resulting in direct conversion of BDFs to myogenic cells.

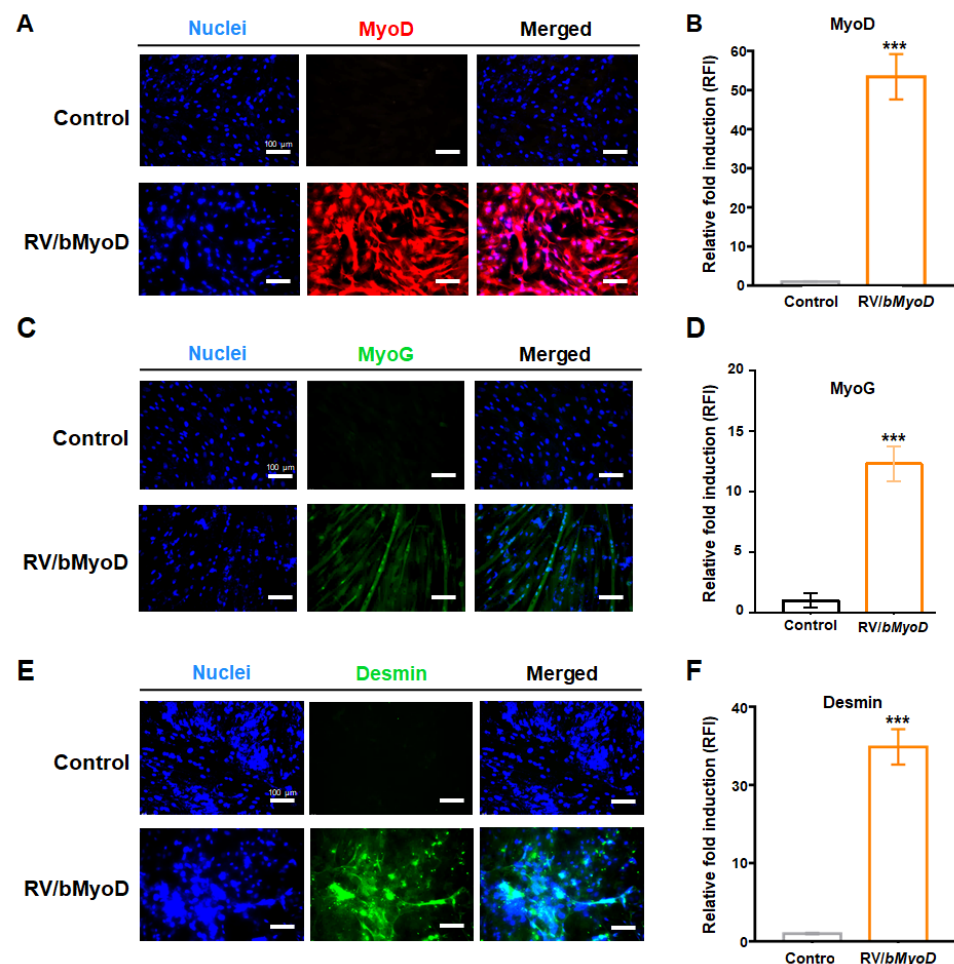


Figure 5. Observation of myogenic protein expression in directly reprogrammed myogenic cells. (A) Immunocytochemical analysis to confirm the expression of MyoD (red fluorescence). (B) Quantified value of MyoD protein expression. (C) Immunocytochemical analysis to confirm the expression of MyoG (green fluorescence). (D) Quantification of MyoG expression. (E) Immunocytochemistry to confirm the expression of Desmin (green fluorescence). (F) Quantification of Desmin expression. $n = 3$ per group. Statistical significance was determined using one-way ANOVA in comparison with the control. *** $p < 0.001$. Scale bars, 100 μm .

4. Discussion

Traditionally, methods for the treatment of damage in muscle tissues include the autografting of patient cells or allografting of donor cells [56,57]. Recently, to overcome limitations derived from the conventional therapeutic approaches, such as stable cell supply problems, multipotential stem-cell-based methods have been studied [10,12]. However, such improved methods still have problems in cost and supply issues, in terms of using stem cells. As an alternative to solve this problem, the utilization of directly reprogrammed muscle cells from other somatic cells has been spotlighted [35,36,58]. According to Wakao et al., in 2017, researchers converted human dermal fibroblasts (HDFs) into myogenic lineage by co-transduction of Mycl and MyoD1 through retrovirus. In 2019, Bnasal et al. converted mouse fibroblasts into skeletal-muscle-like cells through the addition of six small molecules (valproic acid, Chir99021, repsox, forskolin, parnate, and TTNPB) for 9 days. In 2021, Kim et al. converted mouse fibroblasts into induced myogenic progenitor cells. The mouse fibroblasts were isolated from the transgenic mice, in which *Pax7* was overexpressed. Then, the isolated mouse embryonic fibroblasts (MEFs) were transduced by lentivirus, delivering the MyoD gene. After selection of the efficiently transduced MEFs using antibiotics and fluorescence-activated cell sorter (FACS), cells were treated with small molecules (adenylate cyclase activator forskolin, TGF- β receptor inhibitor repsox, and GSK3- β inhibitor Chir99021). Through three steps over 10 days for direct conversion, MEFs showed induced myogenic progenitor cell-like properties. According to these related former studies, two or more factors were needed to generate directly induced myogenic cells from fibroblasts. In addition, most of the studies dealt with human and mouse fibroblasts, contrary to our research handling bovine fibroblasts and bovine MyoD protein and genes.

To promptly generate reprogrammed muscle cells, selection and successful delivery of appropriate transcription factors to somatic cells have been considered to be significant [59,60]. According to recent studies, efficient delivery methods of transcription factors include the most widely used virus-based methods and the recently used cell-permeable protein-based methods. Although the virus-based methods have the advantage of high efficiency, the risk of transgenes has been constantly raised. On the other hand, the methods using cell-penetrating proteins have been suggested to overcome the safety issues, but their efficiency still needs to be improved.

In related studies, MyoD has been studied as an important factor for the direct conversion of human fibroblasts to myoblasts and myotubes [61–63]. According to Berkes et al., MyoD, Myf5, MyoG, and MRF4 have critical roles in skeletal muscle development and these myogenic regulatory factors are responsible for coordinating muscle-specific gene expression in the development of embryos. In this study, we tried to extend the existing results of direct conversion, which are limited to only mouse and human cells, to the results, including cells of domestic animals, especially bovine cells. Therefore, bMyoD was used to directly reprogram the BDFs to bovine myoblasts and myotubes. In the research, the methods for bMyoD delivery were as follows: using a cell-penetrating protein and using a retrovirus. Then, we compared their efficiencies.

For effective gene regulation during cell developments, the stability of transcription factors is one of the most significant properties. However, most transcription factors have been demonstrated to have poor stability. Previously, we reported that 30Kc19-cargo-NLS-R9 protein can be used to deliver cargo proteins into cytoplasm and even into nuclei [49–52]. In addition, the 30Kc19 protein was reported to enhance the stability of transcription factors. Hence, the 30Kc19 protein was determined as a messenger protein to deliver the transcription factor, bMyoD, safely. The results demonstrated that bMyoD conjugated to the 30Kc19 protein, in the form of 30Kc19-bMyoD-NLS-R9 (30MNR), was intracellularly delivered, but did not induce the reprogramming of BDFs (Figure 2). According to immunocytochemistry, bMyoD was successfully transmitted into cells and observed to be localized in nuclei. Based on the transcriptional mechanism of MyoD, which directly binds to a DNA motif, known as E-box, and regulates transcription [64,65], it is difficult to inter-

pret the reason why reprogramming did not occur, even though bMyoD was transmitted into the nuclei. However, since only MyoG was used as a marker of direct conversion, if additional studies can be conducted to precisely examine the actual reprogramming and differentiation, the relationship between the nuclear localization of transcription factor and efficiency of the actual transcription would be revealed for further understanding of the cellular mechanisms.

5. Conclusions

As a result, protein-based direct conversion of BDFs into bovine myoblasts and myotubes using 30MNR was not confirmed; however, the delivery of the bMyoD gene using a retrovirus showed effective direct conversion (Figure 6). For direct reprogramming of myogenic cells using a viral approach, enhanced expression of not only early myogenic markers (MyoD and MyoG), but also late myogenic markers (MYH3, MYMK, Desmin) was significantly observed. Further, the morphological change in cells was clear. In Figure 5A,C,E, though all the cells were experimented on simultaneously with the same condition, cellular morphologies were shown differently, depending upon the staining target. Since the images were obtained by capturing the fluorescence-positive region among the whole cells, it is possible that cells with up-regulated MyoG elongated and fused, resulting in enhanced formation of myotubule structures compared with cells with up-regulated MyoD and Desmin.

Although successful reprogramming was not achieved in cell-penetrating protein-based methods, the 30Kc19 protein enabled mass production of the transcription factor bMyoD in a soluble form, also able to increase the stability of the bMyoD and induce localization into the nuclei. Thus, this study could have important implications in the following research of direct conversion using transgene-free methods, represented as protein-based conversion. Besides, BDFs were successfully converted into myogenic cells by transduction through retrovirus, delivering the bMyoD gene. It would be a great development from the related former studies in terms of diminishing the delivering factor to only one. Moreover, by expanding the results of direct reprogramming from existing murine or human cell-based research to bovine cell-based study, the results could be widely used in the field of not only regenerative medicine but also the cultured meat industry in the future.

A Protein-based direct reprogramming

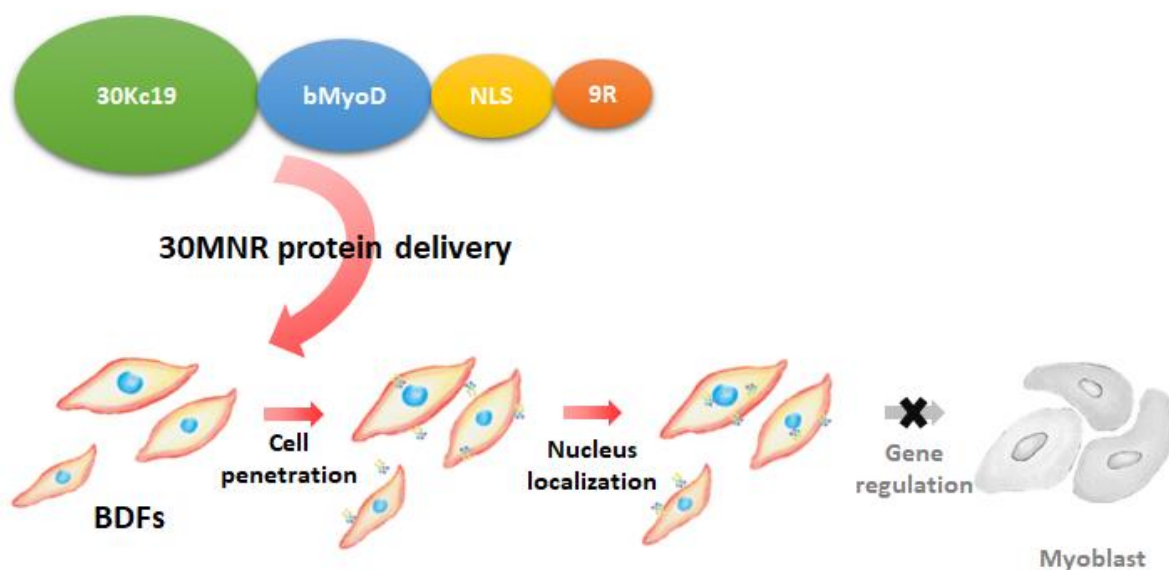


Figure 6. Cont.

B Viral-based direct reprogramming

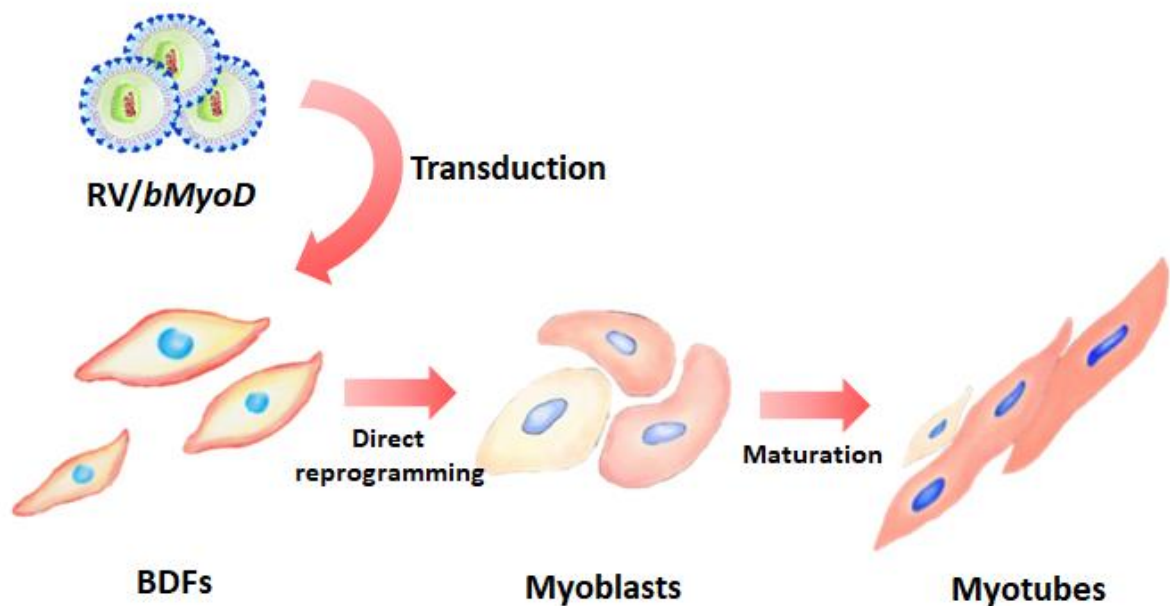


Figure 6. Schematic illustration of direct reprogramming of BDFs into myoblasts or myotubes using viral-based bMyoD delivery. (A) Inefficient method using protein-based approach and (B) efficient method using viral-based approach.

Author Contributions: S.H.L. and S.H. collected data and evidence. B.S., K.S.L. and H.H.P. conceived and designed the study. B.S. and H.H.P. wrote the manuscript. B.S. and S.H.L. drew the figures. B.S., M.K., J.J., K.S.L. and H.H.P. directed and validated the data analysis. All authors have read and agreed to the published version of the manuscript.

Funding: This work was supported by the Korea Evaluation Institute of Industrial Technology (KEIT), grant funded by the Korean Government (MSIT) (No. 20008546). This work was supported by the National Research Foundation of Korea (NRF), grant funded by the Korean Government (MSIT) (No. 2020R1A4A3078645, No. 2022R1A2C1007354).

Institutional Review Board Statement: Not applicable.

Data Availability Statement: The data generated for this study are available on request to the corresponding author.

Conflicts of Interest: The authors declare no conflict of interest.

References

1. Kent-Braun, J.; Ng, A.; Castro, M.; Weiner, M.; Gelinas, D.; Dudley, G.; Miller, R. Strength, skeletal muscle composition, and enzyme activity in multiple sclerosis. *J. Appl. Physiol.* **1997**, *83*, 1998–2004. [[CrossRef](#)] [[PubMed](#)]
2. Pang, Z.P.; Yang, N.; Vierbuchen, T.; Ostermeier, A.; Fuentes, D.; Yang, T.; Citri, A.; Sebastiano, V.; Marro, S.; Südhof, T.; et al. Induction of human neuronal cells by defined transcription factors. *Nature* **2011**, *476*, 220–223. [[CrossRef](#)] [[PubMed](#)]
3. Thier, M.; Wörsdörfer, P.; Lakes, Y.B.; Gorris, R.; Herms, S.; Opitz, T.; Seiferling, D.; Quandt, T.; Hoffmann, P.; Nöthen, M.; et al. Direct conversion of fibroblasts into stably expandable neural stem cells. *Cell Stem Cell* **2012**, *10*, 473–479. [[CrossRef](#)] [[PubMed](#)]
4. Hiramatsu, K.; Sasagawa, S.; Outani, H.; Nakagawa, K.; Yoshikawa, H.; Ysumaki, N. Generation of hyaline cartilaginous tissue from mouse adult dermal fibroblast culture by defined factors. *J. Clin. Investig.* **2011**, *121*, 640–657. [[CrossRef](#)] [[PubMed](#)]
5. Vierbuchen, T.; Ostermeier, A.; Pang, Z.P.; Kokubu, Y.; Südhof, T.; Wernig, M. Direct conversion of fibroblasts to functional neurons by defined factors. *Nature* **2010**, *463*, 1035–1041. [[CrossRef](#)]
6. Xiao, D.; Liu, X.; Zhang, M.; Zou, M.; Deng, Q.; Sun, D.; Bian, X.; Cai, Y.; Guo, Y.; Liu, S.; et al. Direct reprogramming of fibroblasts into neural stem cells by single non-neural progenitor transcription factor Ptf1a. *Nat. Commun.* **2018**, *9*, 1–19. [[CrossRef](#)]
7. Peake, J.M.; Neubauer, O.; Della Gatta, P.A.; Nosaka, K. Muscle damage and inflammation during recovery from exercise. *J. Appl. Physiol.* **2017**, *122*, 559–570. [[CrossRef](#)]

8. Corona, B.T.; Wenke, J.C.; Ward, C.L. Pathophysiology of volumetric muscle loss injury. *Cells Tissues Organs* **2016**, *202*, 180–188. [[CrossRef](#)]
9. Ling, X.F.; Peng, X. What is the price to pay for a free fibula flap? A systematic review of donor-site morbidity following free fibula flap surgery. *Plast. Reconstr. Surg.* **2012**, *129*, 657–674. [[CrossRef](#)]
10. Asakura, A.; Rudnicki, M.A.; Komaki, M. Muscle satellite cells are multipotential stem cells that exhibit myogenic, osteogenic, and adipogenic differentiation. *Differentiation* **2001**, *68*, 245–253. [[CrossRef](#)]
11. Klein, D.; Benchellal, M.; Kleff, V.; Jakob, H.G.; Ergün, S. Hox genes are involved in vascular wall-resident multipotent stem cell differentiation into smooth muscle cells. *Sci. Rep.* **2013**, *3*, 2178. [[CrossRef](#)] [[PubMed](#)]
12. Rodríguez, L.V.; Alfonso, Z.; Zhang, R.; Leung, J.; Wu, B.; Ignarro, L. Clonogenic multipotent stem cells in human adipose tissue differentiate into functional smooth muscle cells. *Proc. Natl. Acad. Sci. USA* **2006**, *103*, 12167–12172. [[CrossRef](#)] [[PubMed](#)]
13. Banks, J.M.; Harley, B.A.; Bailey, R.C. Tunable, photoreactive hydrogel system to probe synergies between mechanical and biomolecular cues on adipose-derived mesenchymal stem cell differentiation. *ACS Biomater. Sci. Eng.* **2015**, *1*, 718–725. [[CrossRef](#)] [[PubMed](#)]
14. Kim, J.H.; Sim, J.; Kim, H.-J. Neural stem cell differentiation using microfluidic device-generated growth factor gradient. *Biomol. Ther.* **2018**, *26*, 380. [[CrossRef](#)] [[PubMed](#)]
15. Pires, F.; Ferreira, Q.; Rodrigues, C.A.; Morgado, J.; Ferreira, F.C. Neural stem cell differentiation by electrical stimulation using a cross-linked PEDOT substrate: Expanding the use of biocompatible conjugated conductive polymers for neural tissue engineering. *Biochim. Biophys. Acta (BBA) Gen. Subj.* **2015**, *1850*, 1158–1168. [[CrossRef](#)]
16. Sarraf, C.; Otto, W.R.; Eastwood, M. In vitro mesenchymal stem cell differentiation after mechanical stimulation. *Cell Prolif.* **2011**, *44*, 99–108. [[CrossRef](#)]
17. Subramony, S.D.; Dargis, B.R.; Castillo, M.; Azeloglu, E.U.; Tracey, M.; Su, A.; Lu, H. The guidance of stem cell differentiation by substrate alignment and mechanical stimulation. *Biomaterials* **2013**, *34*, 1942–1953. [[CrossRef](#)]
18. Tomaskovic-Crook, E.; Gu, Q.; Rahim, S.N.A.; Wallace, G.G.; Crook, J.M. Conducting polymer mediated electrical stimulation induces multilineage differentiation with robust neuronal fate determination of human induced pluripotent stem cells. *Cells* **2020**, *9*, 658. [[CrossRef](#)]
19. Wang, Y.K.; Chen, C.S. Cell adhesion and mechanical stimulation in the regulation of mesenchymal stem cell differentiation. *J. Cell. Mol. Med.* **2013**, *17*, 823–832. [[CrossRef](#)]
20. Chen, L.; Liu, J.; Guan, M.; Zhou, T.; Duan, X.; Xiang, Z. Growth factor and its polymer scaffold-based delivery system for cartilage tissue engineering. *Int. J. Nanomed.* **2020**, *15*, 6097. [[CrossRef](#)]
21. Gotoh, N. Regulation of growth factor signaling by FRS2 family docking/scaffold adaptor proteins. *Cancer Sci.* **2008**, *99*, 1319–1325. [[CrossRef](#)] [[PubMed](#)]
22. Han, U.; Park, H.H.; Kim, Y.J.; Park, T.H.; Park, J.H.; Hong, J.K. Efficient encapsulation and sustained release of basic fibroblast growth factor in nanofilm: Extension of the feeding cycle of human induced pluripotent stem cell culture. *ACS Appl. Mater. Interfaces* **2017**, *9*, 25087–25097. [[CrossRef](#)] [[PubMed](#)]
23. Driscoll, D.; Farnia, S.; Kefalas, P.; Maziarsz, R.T. Concise review: The high cost of high tech medicine: Planning ahead for market access. *Stem Cells Transl. Med.* **2017**, *6*, 1723–1729. [[CrossRef](#)] [[PubMed](#)]
24. Okita, K.; Ichisaka, T.; Yamanaka, S. Generation of germline-competent induced pluripotent stem cells. *Nature* **2007**, *448*, 313–317. [[CrossRef](#)] [[PubMed](#)]
25. Takahashi, K.; Yamanaka, S. Induction of pluripotent stem cells from mouse embryonic and adult fibroblast cultures by defined factors. *Cell* **2006**, *126*, 663–676. [[CrossRef](#)] [[PubMed](#)]
26. Ieda, M.; Fu, J.-D.; Delgado-Olguin, P.; Vedantham, V.; Hayashi, Y.; Bruneau, B.; Srivastava, D. Direct reprogramming of fibroblasts into functional cardiomyocytes by defined factors. *Cell* **2010**, *142*, 375–386. [[CrossRef](#)] [[PubMed](#)]
27. Kim, J.; Efe, J.A.; Zhu, S.; Talantova, M.; Yuan, X.; Wang, S.; Lipton, S.; Zhang, K.; Ding, S. Direct reprogramming of mouse fibroblasts to neural progenitors. *Proc. Natl. Acad. Sci. USA* **2011**, *108*, 7838–7843. [[CrossRef](#)]
28. Szabo, E.; Rampalli, S.; Risueno, R.M.; Schnerch, A.; Mitchell, R.; Fiebig-Comyn, A.; Levadoux-Martin, M.; Bhatia, M. Direct conversion of human fibroblasts to multilineage blood progenitors. *Nature* **2010**, *468*, 521–526. [[CrossRef](#)]
29. Chang, Y.; Lee, E.; Kim, J.; Kwon, Y.-W.; Kwon, Y.; Lim, J. Efficient in vivo direct conversion of fibroblasts into cardiomyocytes using a nanoparticle-based gene carrier. *Biomaterials* **2019**, *192*, 500–509. [[CrossRef](#)]
30. Ifkovits, J.L.; Addis, R.C.; Epstein, J.A.; Gearhart, J.D. Inhibition of TGF β signaling increases direct conversion of fibroblasts to induced cardiomyocytes. *PLoS ONE* **2014**, *9*, e89678. [[CrossRef](#)]
31. Pfisterer, U.; Kirkeby, A.; Torper, O.; Wood, J.; Nelander, J.; Dufour, A.; Björklund, A.; Lindvall, O.; Jakobsson, J.; Parmar, M. Direct conversion of human fibroblasts to dopaminergic neurons. *Proc. Natl. Acad. Sci. USA* **2011**, *108*, 10343–10348. [[CrossRef](#)] [[PubMed](#)]
32. Torper, O.; Pfisterer, U.; Wolf, D.A.; Pereira, M.; Lau, S.; Jakobsson, J.; Björklund, A.; Grealish, S.; Parmar, M. Generation of induced neurons via direct conversion in vivo. *Proc. Natl. Acad. Sci. USA* **2013**, *110*, 7038–7043. [[CrossRef](#)] [[PubMed](#)]
33. Shi, J.-W.; Zhang, T.-T.; Liu, W.; Yang, J.; Lin, X.-L.; Jia, J.-S.; Shen, H.-F.; Wang, S.-C.; Li, J.; Zha, W.-T.; et al. Direct conversion of pig fibroblasts to chondrocyte-like cells by c-Myc. *Cell Death Discov.* **2019**, *5*, 126. [[CrossRef](#)] [[PubMed](#)]
34. Takimoto, A.; Oro, M.; Hiraki, Y.; Shukunami, C. Direct conversion of tenocytes into chondrocytes by Sox9. *Exp. Cell Res.* **2012**, *318*, 1492–1507. [[CrossRef](#)]

35. Kim, I.; Ghosh, A.; Bundschuh, N.; Hinte, L.; Von Meyenn, F.; Bar-Nur, O. Integrative molecular roadmap for direct conversion of fibroblasts into myocytes and myogenic progenitor cells. *bioRxiv* **2021**, 2–7. [[CrossRef](#)]
36. Wakao, J.; Kishida, T.; Fumino, S.; Kimura, K.; Yamamoto, K.; Kotani, S.; Mizuyshima, L.; Naito, Y.; Yoshikawa, T.; Tajiti, T.; et al. Efficient direct conversion of human fibroblasts into myogenic lineage induced by co-transduction with MYCL and MYOD1. *Biochem. Biophys. Res. Commun.* **2017**, *488*, 368–373. [[CrossRef](#)]
37. Dey, C.; Narayan, G.; Krishna Kumar, H.; Borgohain, M.P.; Lenka, N.; Thummer, R. Thummer. Cell-Penetrating Peptides as a Tool to Deliver Biologically Active Recombinant Proteins to Generate Transgene-Free Induced Pluripotent Stem Cells. *Stud. Stem Cells Res. Ther.* **2016**, *3*, 006–015. [[CrossRef](#)]
38. Liu, H.; Zeng, F.; Zhang, M.; Huang, F.; Wang, J.; Guo, J.; Liu, C.; Wang, H. Emerging landscape of cell penetrating peptide in reprogramming and gene editing. *J. Control. Release* **2016**, *226*, 124–137. [[CrossRef](#)]
39. Seo, B.J.; Hong, Y.J.; Do, J.T. Cellular reprogramming using protein and cell-penetrating peptides. *Int. J. Mol. Sci.* **2017**, *18*, 552. [[CrossRef](#)]
40. Takashina, T.; Koyama, T.; Nohara, S.; Hasegawa, M.; Ishiguro, A.; Iijima, K.; Lu, J.; Shimura, M.; Okamura, T.; Sakuma, T.; et al. Identification of a cell-penetrating peptide applicable to a protein-based transcription activator-like effector expression system for cell engineering. *Biomaterials* **2018**, *173*, 11–21. [[CrossRef](#)]
41. Motohashi, T.; Kunisada, T. Direct conversion of mouse embryonic fibroblasts into neural crest cells. In *Skin Stem Cells*; Springer: Berlin/Heidelberg, Germany, 2018; pp. 307–321.
42. Sowa, Y.; Kishida, T.; Tomita, K.; Yamamoto, K.; Numajiri, T.; Mazda, O. Direct conversion of human fibroblasts into Schwann cells that facilitate regeneration of injured peripheral nerve in vivo. *Stem Cells Transl. Med.* **2017**, *6*, 1207–1216. [[CrossRef](#)] [[PubMed](#)]
43. Hoshiba, T.; Yokoyama, N. Decellularized extracellular matrices derived from cultured cells at stepwise myogenic stages for the regulation of myotube formation. *Biochim. Biophys. Acta (BBA) Mol. Cell Res.* **2020**, *1867*, 118658. [[CrossRef](#)] [[PubMed](#)]
44. Li, H.; Choudhary, S.K.; Milner, D.J.; Munir, M.I.; Kuisk, I.R.; Capetanaki, Y. Inhibition of desmin expression blocks myoblast fusion and interferes with the myogenic regulators MyoD and myogenin. *J. Cell Biol.* **1994**, *124*, 827–841. [[CrossRef](#)] [[PubMed](#)]
45. Muscaritoli, M.; Anker, S.; Argiles, J.; Aversa, Z.; Bauer, J.M.; Biolo, G.; Boirie, Y.; Bosaeus, I.; Cederholm, T.; Costelli, P.; et al. Consensus definition of sarcopenia, cachexia and pre-cachexia: Joint document elaborated by Special Interest Groups (SIG) “cachexia-anorexia in chronic wasting diseases” and “nutrition in geriatrics”. *Clin. Nutr.* **2010**, *29*, 154–159. [[CrossRef](#)] [[PubMed](#)]
46. Bhat, Z.F.; Fayaz, H. Prospectus of cultured meat—advancing meat alternatives. *J. Food Sci. Technol.* **2011**, *48*, 125–140. [[CrossRef](#)]
47. Stephens, N.; Di Silvio, L.; Dunsford, I.; Ellis, M.; Glencross, A.; Sexton, A. Bringing cultured meat to market: Technical, socio-political, and regulatory challenges in cellular agriculture. *Trends Food Sci. Technol.* **2018**, *78*, 155–166. [[CrossRef](#)]
48. Lee, H.J.; Park, H.H.; Kim, J.A.; Park, J.H.; Ryu, J.; Choi, J.; Lee, J.; Rhee, W.J.; Park, T.H. Enzyme delivery using the 30Kc19 protein and human serum albumin nanoparticles. *Biomaterials* **2014**, *35*, 1696–1704. [[CrossRef](#)]
49. Lee, J.; Park, H.H.; Park, J.H. Efficient production of cell-permeable oct4 protein using 30Kc19 protein originating from silkworm. *Biotechnol. Bioprocess Eng.* **2019**, *24*, 964–971. [[CrossRef](#)]
50. Park, H.H.; Sohn, Y.; Yeo, J.W.; Park, J.H.; Lee, H.J.; Ryu, J.; Rhee, W.J.; Park, T.H. Identification and characterization of a novel cell-penetrating peptide of 30Kc19 protein derived from *Bombyx mori*. *Process Biochem.* **2014**, *49*, 1516–1526. [[CrossRef](#)]
51. Park, J.H.; Lee, J.H.; Park, H.H.; Rhee, W.J.; Choi, S.S.; Park, T.H. A protein delivery system using 30Kc19 cell-penetrating protein originating from silkworm. *Biomaterials* **2012**, *33*, 9127–9134. [[CrossRef](#)]
52. Ryu, J.; Park, H.H.; Park, J.H.; Lee, H.J.; Rhee, W.J.; Park, T.H. Soluble expression and stability enhancement of transcription factors using 30Kc19 cell-penetrating protein. *Appl. Microbiol. Biotechnol.* **2016**, *100*, 3523–3532. [[CrossRef](#)] [[PubMed](#)]
53. Guo, X.; Badu-Mensah, A.; Thomas, M.C.; McAleer, C.W.; Hickman, J.J. Characterization of functional human skeletal myotubes and neuromuscular junction derived—from the same induced pluripotent stem cell source. *Bioengineering* **2020**, *7*, 133. [[CrossRef](#)] [[PubMed](#)]
54. Pircher, T.; Wackerhage, H.; Akova, E.; Böcker, W.; Aszodi, A.; Saller, M. Fusion of Normoxic-and Hypoxic-Preconditioned Myoblasts Leads to Increased Hypertrophy. *Cells* **2022**, *11*, 1059. [[CrossRef](#)] [[PubMed](#)]
55. Yuzawa, R.; Koike, H.; Manabe, I.; Oishi, Y. VDR regulates simulated microgravity-induced atrophy in C2C12 myotubes. *Sci. Rep.* **2022**, *12*, 1377. [[CrossRef](#)]
56. Li, M.T.A.; Willett, N.J.; Uhrig, B.A.; Guldborg, R.E.; Warren, G.L. Functional analysis of limb recovery following autograft treatment of volumetric muscle loss in the quadriceps femoris. *J. Biomech.* **2014**, *47*, 2013–2021. [[CrossRef](#)]
57. Norris, R.; Glasby, M.; Gattuso, J.; Bowden, R. Peripheral nerve repair in humans using muscle autografts. A new technique. *J. Bone Jt. Surg. Br. Vol.* **1988**, *70*, 530–533. [[CrossRef](#)]
58. Bansal, V.; De, D.; An, J.; Kang, T.M.; Jeong, H.-J.; Kang, J.-S.; Lim, K.K. Chemical induced conversion of mouse fibroblasts and human adipose-derived stem cells into skeletal muscle-like cells. *Biomaterials* **2019**, *193*, 30–46. [[CrossRef](#)]
59. Lee, K.; Rafi, M.; Wang, X.; Aran, K.; Feng, X.; Sterzo, C.; Tang, R.; Lingampalli, N.; Kim, H.J.; Murthy, N. In vivo delivery of transcription factors with multifunctional oligonucleotides. *Nat. Mater.* **2015**, *14*, 701–706. [[CrossRef](#)]
60. Rilo-Alvarez, H.; Ledo, A.M.; Vidal, A.; Garcia-Fuentes, M. Delivery of transcription factors as modulators of cell differentiation. *Drug Deliv. Transl. Res.* **2021**, *11*, 426–444. [[CrossRef](#)]
61. Berkes, C.A.; Tapscott, S.J. *Seminars in Cell & Developmental Biology*; Elsevier: Amsterdam, The Netherlands, 2005; pp. 585–595.
62. Hollenberg, S.M.; Cheng, P.F.; Weintraub, H. Use of a conditional MyoD transcription factor in studies of MyoD trans-activation and muscle determination. *Proc. Natl. Acad. Sci. USA* **1993**, *90*, 8028–8032. [[CrossRef](#)]

63. Rudnicki, M.A.; Jaenisch, R. The MyoD family of transcription factors and skeletal myogenesis. *Bioessays* **1995**, *17*, 203–209. [[CrossRef](#)] [[PubMed](#)]
64. Heidt, A.B.; Rojas, A.; Harris, I.S.; Black, B.L. Determinants of myogenic specificity within MyoD are required for noncanonical E box binding. *Mol. Cell. Biol.* **2007**, *27*, 5910–5920. [[CrossRef](#)] [[PubMed](#)]
65. Shklover, J.; Etzioni, S.; Weisman-Shomer, P.; Yafe, A.; Bengal, E.; Fry, M. MyoD uses overlapping but distinct elements to bind E-box and tetraplex structures of regulatory sequences of muscle-specific genes. *Nucleic Acids Res.* **2007**, *35*, 7087–7095. [[CrossRef](#)] [[PubMed](#)]